DEVELOPMENT OF A TIME-OF-FLIGHT COMPTON CAMERA FOR ONLINE CONTROL OF ION THERAPY

J.-L. Ley[1], C. Abellan[2], J.-P. Cachemiche[2], M. Dahoumane[1], D. Dauvergne[1], N. Freud[3], B. Joly[4], J. Krimmer[1], L. Lestand[4], J.M. Létang[3], H. Mathez[1], V. Maxim[3], G. Montarou[4], C. Ray[1], M-H Richard[1], E. Testa[1], Y. Zoccarato[1]

[1] Institut de Physique Nucléaire de Lyon; [2] CPPM, Aix-Marseille Université, CNRS/IN2P3, Marseille; [3] Laboratoire CREATIS, Lyon; [4] Laboratoire de Physique Corpusculaire de Clermont-Ferrand

COMPTON CAMERA

PURPOSE

The aim of irradiation monitoring during a treatment in ion therapy is to control in real time the agreement between the delivered dose and the planned treatment. In fact, the discrepancies might come from uncertainties such as the positioning or the morphological changes of the patient. They can lead to ion-range variations of a few millimeters. Several devices are under development over the world to detect secondary radiations, which are correlated to the dose deposited by incident ions. Compton cameras are in particular investigated for their potential high efficiency to detect prompt gamma rays [1,2,3,4]. The present work aims at discussing the clinical applicability of a Compton camera design by means of Monte Carlo simulations for proton and carbon ion therapy.

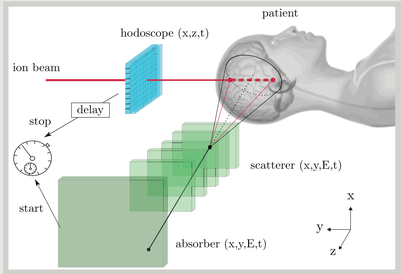

Fig. 1. Configuration of the monitoring system: the prompt gamma-ray emission points are reconstructed by intersecting the ion trajectory and the Compton cone. The ion trajectory is obtained with the hodoscope and the Compton cone is reconstructed with the camera. Time of flight (TOF) measurements between the absorber detector and the beam hodoscope (with an appropriate delay) are performed. [5]

SIMULATIONS GEANT4.9.6

KEY POINTS

- Monte-Carlo simulation: Geant4.9.6
- Use the standard electromagnetic processes and the Binary Cascade model for hadrons
- Taking account of the Doppler broadening and polarization
- Cut at 0.1 mm in PMMA and 1 mm in the detectors

	Protons	Carbon ions
Number	10^8	4 x 10^7
Energy	160 MeV	305 MeV/u
Bragg peak position	15.5 cm	

Table 1. Parameters used for the simulation of the Compton camera.

Resolution (FWHM) @ 1 MeV	BGO	Si
Spatial [mm]	5	0.9
Energy [%]	17	2.3
Timing [ns]	3	15

Table 2. Realistic resolutions defined in the simulations for the detectors. The energy resolution for the silicon is defined with the Equivalent Noise Charge (ENC). The ENC for the silicon is expected to be 200.

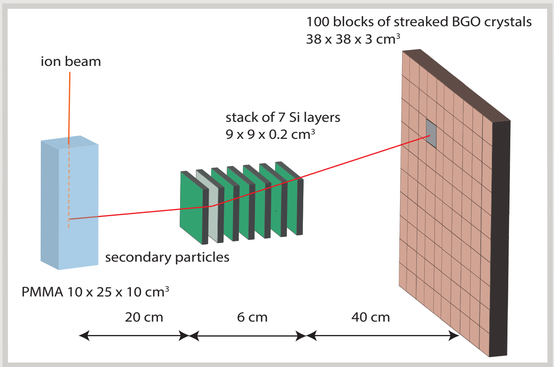

Fig. 2. Diagram of the simulation setup.

DATA TREATMENT

A beam time structure is modeled and applied to the simulation data in order to estimate the coincidence rate (true/random) for a clinical application of the Compton camera. The treatment is done for protons and carbon ions.

		Protons	Carbon ions
CLINICAL CHARACTERISTICS	**Facility**	Cyclotron C230 IBA	Synchroton at HIT
	Clinical intensity	2 x 10^{10} p/s	5 x 10^7 ions/s
	Energy	160 MeV	305 MeV/u
BEAM STRUCTURE	**Bunch time [ns]**	3.2	30
	Period [ns]	9.4	170
	Particles / bunch	217	9
DETECTORS	**Coincidence window [ns]**	40	40

Table 3. Characteristics of clinical beams using protons and carbon ions. Each particle is treated as an individual story in the simulation Geant4.The beam time strucure is modeled in the simulation data analysis.

RESULTS

			COINCIDENCE RATE FOR PROTONS						COINCIDENCE RATE FOR CARBON IONS			
Structure			**Single proton**		**IBA**				**Single ion**		**HIT**	
Intensity			10^6 p/s		1.2 x 10^9 p/s		2 x 10^{10} p/s		10^6 ion/s		5 x 10^7 ions/s	
Detectors			perfect	real	perfect	real	perfect	real	perfect	real	perfect	real
Coincidence [%]	**Random**		0	0	0.3	47.1	7.1	92.3	≈ 0	8.9 x 10^{-2}	4.7	64.0
	True	**all**	100	100	99.7	52.9	92.9	7.7	≈100	99.9	95.3	36.0
		same gamma	92.0	51.5	91.7	27.3	85.5	2.9	84.6	22.5	80.6	7.7
		other	8.0	48.5	8.0	25.6	7.4	3.8	15.4	77.4	14.7	28.3
Count rate coincidence [MHz]			/	/	7.7 x 10^{-2}	0.2	4.7	15.3	/	/	0.03	0.3
Count rate single [MHz]	**1st silicon layer**		/	/	1.4		22.7		/	/	1	
	absorber		/	/	16.8		281		/	/	8.1	

Table 4. The relative coincidence rates are given for three different proton and carbon ion intensities. There are no cuts in energy or with time of flight. The count rate is the sum of the random and the true coincidences. The count rate single is the number of particles which deposit energy in the detector independently of a coincidence. The first silicon layer has the highest single count rate.

COINCIDENCE

Coincidence: one energy deposit in the BGO absorber and one (only one) energy deposit in a Si of the scatterer.
Random coincidence: the energy deposits in the scatterer and the absorber are induced by radiations coming from 2 different incident particles (on the target).
True coincidence: the energy deposits in the scatterer and the absorber are induced by one or several radiations coming from a single incident particle.

- **same gamma:** a true coincidence coming from the same gamma in Si and BGO.
- **other:** the other possibilities for a true coincidence are :
  - two different kinds of particles
  - two different gamma rays
  - same particle but different than gamma

RECONSTRUCTION METHOD

The reconstruction method chosen to get the falloff position is the line-cone method. This method calculates the intersection between a line (trajectory of the incident particle on the target) and a cone (the Compton cone): there are two solutions. Some coincidences have no solutions with this method. Therefore, there is a difference between the coincidence rates in table 4 and the number of reconstructed coincidences due to the solutions allowed by the line-cone method. There are three times less events in the profile than the number of coincidences. Moreover, only the closest solution to the falloff is taken into account.

DEFINITIONS

STRUCTURE

Single particle: One particle is run each microsecond
IBA or HIT: Application of the specific time beam structure

DETECTORS

Perfect: no timing resolution is applied. The time window defined to detect a coincidence is the time for a photon to fly from the silicon layer to the absorber.
Real: a realistic timing resolution is applied to the detectors (table 3) and the time window for a coincidence is set at 40 ns.

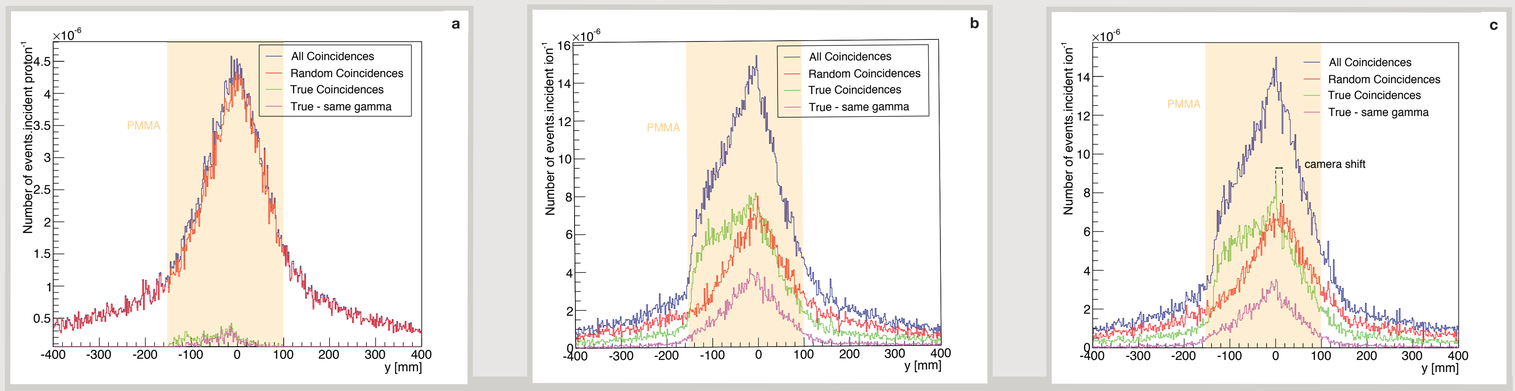

Fig. 4. Reconstructed profile in the case of protons (a) and carbon ions (b,c) with the time structure of the beam and realistic detector resolutions. The theoretical falloff position is 0 mm along the Y axis. For the figure 4a and 4b, the camera is centred on the Bragg peak position. In the figure 4c, the camera is shifted to 50 mm after the Bragg peak position. It shows that the maximum of the random coincidence distrubution is due to the position of the camera and not related to the falloff position. Therefore, we have to distinguish true coincidences which are the only way to get the falloff position.

DISCUSSION

PROTONS

- The fraction of random coincidences is about 90 % with a clinical beam and realistic detectors.
  This can be explained by:
  The beam structure: The number of protons per bunch at 2 x 10^{10} p/s is 217. Therefore, there is a large amount of secondary particles at the same time that contribute to the random coincidences.
  The timing resolution of silicon: The 15 ns induce a large uncertainty on the real interaction time and require a large coincidence window.
- Possibilities to improve the rate of true coincidences:
  Cuts in deposited energy: An analysis on the deposited energies in the detectors was made in order to eliminate the coincidences due to charged particles. It works well for high energy (deposited energy >10 MeV in BGO and > 1 MeV in Si). However, the ratio between true and random coincidences is not improved because the majority of the random coincidences deposit a small amount of energy. It appears that the energy selection is not sufficient to improve the fraction of true coincidences.
  Use of the time of flight information: The time of flight between the hodoscope and the absorber (or using the cyclotron HF signal) could help to differenciate gamma which are faster than neutrons or protons.
  Smaller coincidence window: The fraction of random coincidences reduced to ~10% with a perfect detectors which let some perspectives for Compton camera using very fast detectors.
  Increase distance: at 1 meter, the random coincidences are divided by a factor 50, whereas the true coincidences are only divided by 10. However, with only 1.1 x 10^5 true coincidences per second, we will no longer be able to reach the desired statistics for a beam spot.
- Conclusion:
  For a clinical beam intensity (2 x 10^{10} p/s) with these detectors and this setup, the number of protons in a bunch is too high. The true coninicidences are completely dominated by the random coincidences. A solution could be, at least, to decrease the intensity for the distal spots and then to have a higher intensity beam for the rest of the tumor. With the diminution of the clinical intensity, the quality assurance could be possible in real time with this Compton camera.

CARBON IONS

- The coincidence rate is more favorable for carbon ions thanks to the lower beam intensity.
- The data analysis is still under progress. The number of neutrons and protons generated by nuclear reactions is high. Therefore, we expect that the time of flight information will improve the rate of true coincidences.
- The Compton camera applicability for carbon ion therapy seems more realistic.

RECONSTRUCTION

With a standard MLEM reconstruction algorithm, the source distribution is reconstructed by intersecting all the Compton cones together. Some of the cone intersections do not correspond to an actual source position. These points are eliminated by the iteration process. This should improve the reconstruction of the falloff position [6].

PROTOTYPE DEVELOPMENT

THERE ARE THREE PARTS:

1. Hodoscope → Poster 32 (J. Krimmer)

- Scintillating square fibers: 140 x 1 x 1 mm³
- Number of fibers: 2 x 128
- 8 PMTs Hamamatsu multianodes H8500
- Timing resolution: 1 ns
- Count rate: 10^8 counts/s

2. Scatterer (Double-sided silicon strip detector)

- Number of layers: 7
- Dimensions: 90 x 90 x 2 mm³
- Number of strips: 2 x 64
- Pitch: 1.4 mm
- Expected performances
  - Spatial resolution: 1 mm
  - Energy resolution: 2 keV (FWHM) @ 1 MeV

3. Absorber (streaked BGO)

- Dimensions: 380 x 355 x 30 mm³
- Number of blocks: 96
- 4 PMTs per block
- Timing resolution: 3 ns
- Spatial resolution: 4 mm

4. µTCA acquisition system → Poster 3 (C. Abellan)

- Communication between the µTCA and the acquisition computer thanks to a gigabit ethernet link.

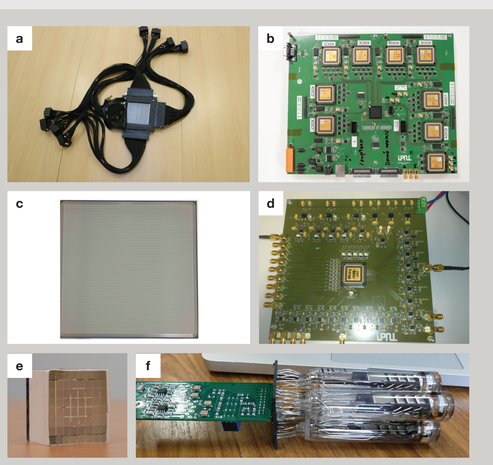

Fig. 5. a. The hodoscope with its 512 optical fibers connected
b. Front End card for a first hodoscope prototype 2 x 32 fibers
c. Double-sided silicon strip detector
d. First prototype of an ASIC for the DSSD's front end
e. BGO block (96 blocks compose the absorber)
f. Each block is connected to 4 PMTs

REFERENCES

[1] S.W. Peterson et al., Phys. Med. Biol. 55 (2010) 6841–6856
[2] G. Llosa et al., NIMA 695(2012)105–108
[3] T. Kormoll et al., IEEE-TNS (2011) 3484 - 3487
[4] S. Kurosawa et al., Current Applied Physics 12 (2012) 364-368
[5] M.-H. Richard et al, IEEE-NSS/MIC (2011) 3496-3500
[6] X. Lojacono et al, IEEE-TNS (2013) 3355 - 3363

CONTACT

Jean-Luc Ley
PhD Student
Mail: ley@ipnl.in2p3.fr
Tel: +33 (0)4 72 43 14 81